MRI in a magnetized Taylor-Couette flow — preparatory studies for upcoming DRESDYN-MRI experiments

George Mamatsashvili

Helmholtz-Zentrum Dresden-Rossendorf (HZDR)

Co-authors: Ashish Mishra & Frank Stefani (HZDR)

This work was supported by Shota Rustaveli National Science Foundation of Georgia (SRNSFG) [#FR-23-1277]

HELMHOLTZ
ZENTRUM DRESDEN
ROSSENDORF

Outline

- MRI: from astrophysics to laboratory
- DRESDYN facility at HZDR
- Theoretical results on the linear and nonlinear dynamics of MRI for the upcoming DRESDYN-MRI experiments
- Summary and future work

Magnetorotational Instability (MRI)

Magnetorotational instability (MRI) is a powerful dynamical instability arising as a result of the combined effects of differential rotation (shear) and a background magnetic field

MRI is amongst the most important instabilities in astrophysics, driving angular momentum transport, dynamo and mass transport in accretion disks and stars

AD around Black Hole (NASA)

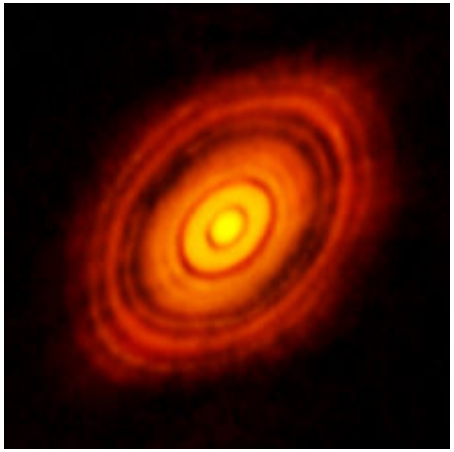

ALMA image of HL Tauri (Mueller et al. 2018)

Structure of MRI-turbulence

Sustained MHD turbulence driven by MRI was first demonstrated in the 90s via simulations in the shearing box model and extensively studied by many groups since then

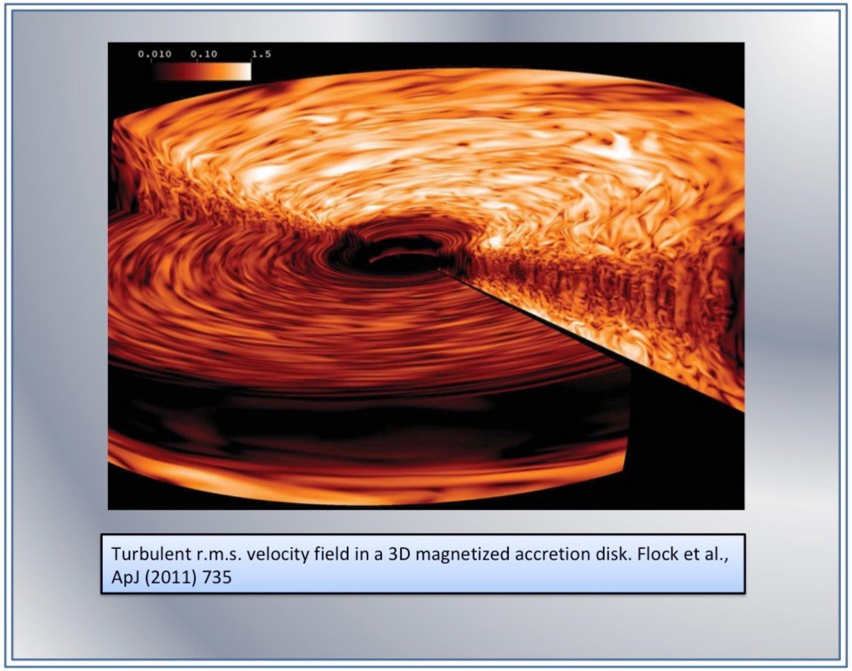

Flock et al. (2011)

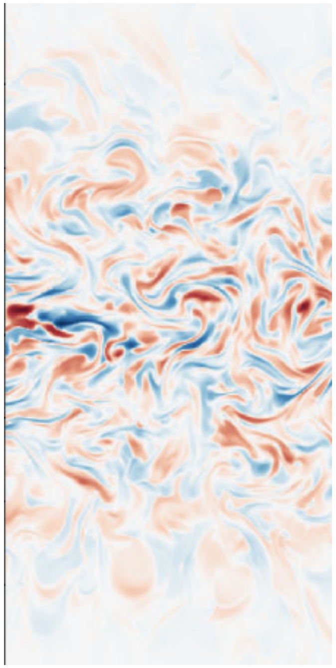

Held et al. (2024)

Turbulence is magnetically dominated — predominantly Maxwell stress of the turbulent magnetic field is responsible for most of outward transport of angular momentum and hence mass accretion

MRI in the laboratory

Interest and efforts in the laboratory detection and studies of MRI since the 2000s

Taylor-Couette (TC) flow threaded by an external magnetic field is a basic setup used in MRI-experiments in the laboratory due to its analogy with accretion disks

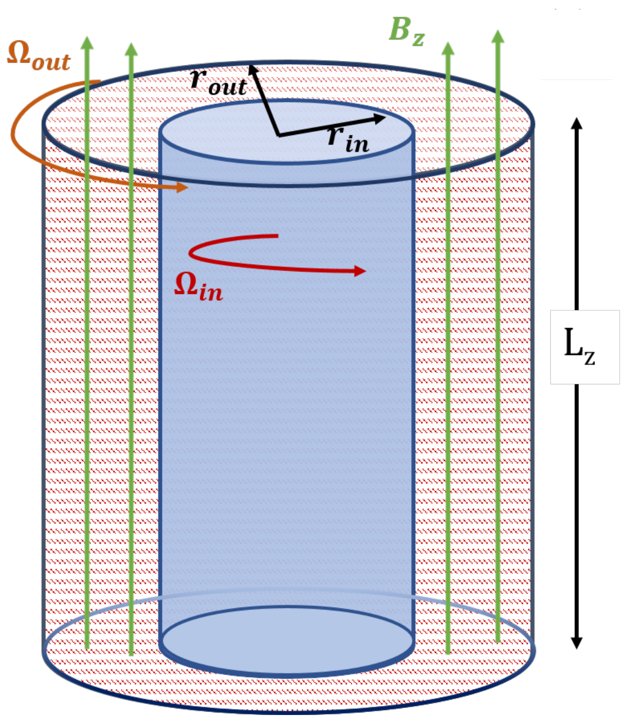

Woking substance: liquid metals (GaInSn, Sodium) with very small magnetic Prandtl numbers

$$Pm = \nu/\eta \sim 10^{-6} - 10^{-5}$$

ν– viscosity
η– magnetic diffusivity

Previous theory and experiments on MRI in TC flows

The first linear analysis of MRI with an imposed constant vertical magnetic field B_{0z} so-called **Standard MRI (SMRI)**, in viscous and resistive TC flows theoretically showed its plausibility under laboratory conditions in the 2000s

(e.g., Ji et al. 2001, Goodman & Ji 2002, Rüdiger et al. 2003)

Moreover, i**nductionless** forms of MRI were revealed in these TC flows:

— **Helical MRI (HMRI)** with an imposed helical $B_{0\phi} + B_{0z}$ magnetic fields

(Hollerbach & Rüdiger 2005, Liu et al. 2006, Priede 2007)

— **Azimuthal MRI (AMRI)** with an imposed $B_{0\phi}$ azimuthal field

(Rüdiger et al. 2007, Hollerbach et al. 2010)

Maryland MRI-exp.

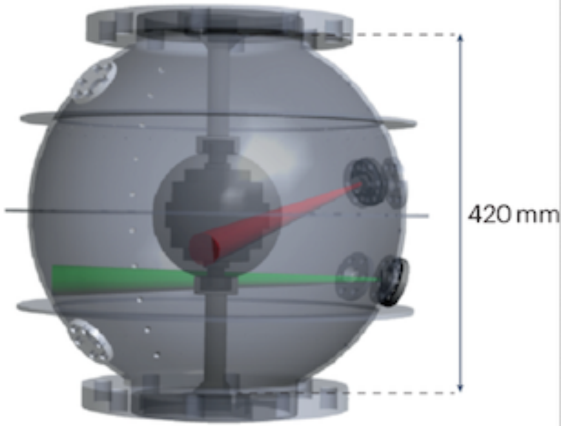

Claimed MRI detection but in fact turned to be Shercliff layer instability (Sisan et al. 2004)

Princeton MRI-exp.

Detected magnetocoriolis waves/Shercliff layer instability, (Nornberg et al. 2010
Roach et al. 2012
Caspary et al. 2018
Wang et al. 2022)

PROMISE

Detected HMRI, AMRI and Tayler instability (Stefani et al. 2006, 2009
Seilmayer et al. 2012, 2014)

SMRI could NOT be definitively detected by that time — the main challenge was to reach high enough magnetic Reynolds numbers *Rm* ~10 and field strength needed for the excitation of SMRI, resulting in very high Reynolds numbers *Re* ~ 10^6 due to very small $Pm = \nu/\eta = Rm/Re \lesssim 10^{-5}$ of liquid metals

In 2022, **the Princeton group** (Wang et al. 2022) found some experimental evidence for axisymmetric and non-axisymmetric SMRI, **BUT**

— the detected instabilities occur at much lower critical $Rm_c \sim 3$ **and axial field** $B_{0z,c} \sim 2000G$ **than linear analysis in the classical TC flow predicts** $Rm_c \sim 10,\ B_{0z,c} \sim 5000G$

(Mishra et al. 2022, Rüdiger & Schultz 2024)

— axisymmetric and non-axisymmetric unstable modes appear very close to each other in the $(Rm,\ B_{0z})$ **- plane**

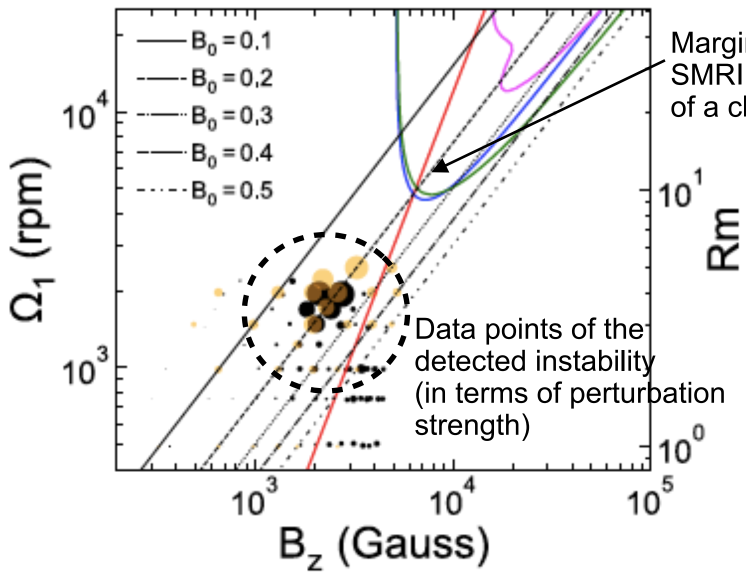

Wang et al. (2022)

These experimental findings on SMRI detection although quite promising, are still tentative, which should be confirmed and further studied/clarified

DRESDYN Project

New generation of precession dynamo and MRI experiments at HZDR

DRESDYN — DREsden Sodium facility for DYNamo studies — is a platform for large-scale liquid sodium experiments devoted to fundamental geo- and astrophysical as well as to various applied problems

Stefani et al.: Geophys. Astrophys. Fluid Dyn. (2019)

Precession dynamo experiment

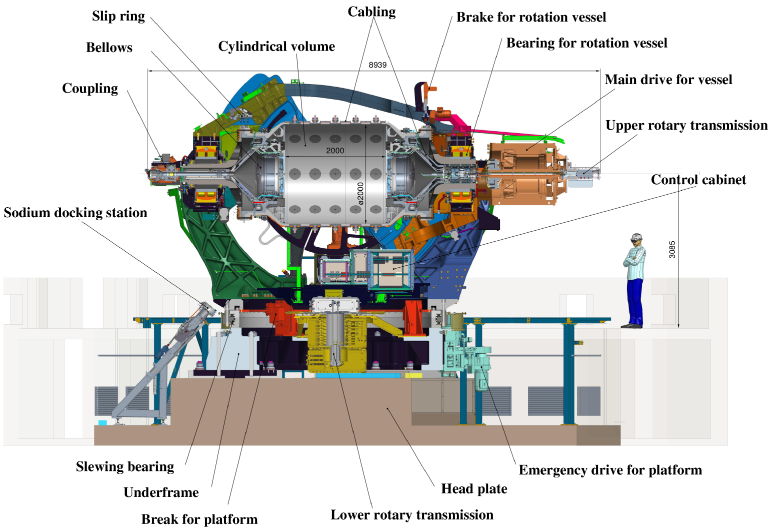

MRI/TI experiment

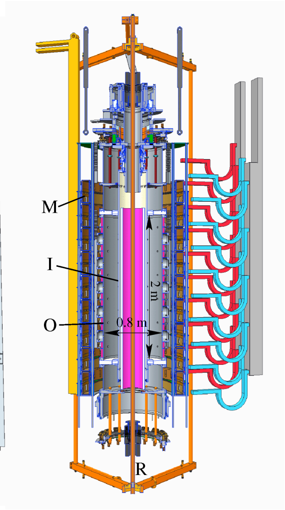

The new big, advanced TC device in DRESDYN

Physical Parameter	Values
r_{in}	0.2 m
r_{out}	0.4 m
L_z	2 m
Ω_{in}	$\leq 2\pi \cdot 20$ Hz
Ω_{out}	$\leq 2\pi \cdot 6$ Hz
Axial magnetic field (B_{0z})	≤ 150 mT
Current through central rod (I)	≤ 50 kA
Conductivity (σ)	$9.5 \times 10^6 S/m$
Viscosity(ν)	$6.512 \times 10^{-7} m^2/s$
Density (ρ)	$920\ kg/m^3$

Physical parameters of the DRESDYN MRI-experiment

Dimensionless Parameter	Definition	Values
μ	Ω_{out}/Ω_{in}	(0.25,0.35]
β	$B_{0\phi}(r_{in})/B_{0z}$	[0, 4]
Normalised height of the TC device	L_z/r_{in}	10
Renolds number (*Re*)	$\Omega_{in} r_{in}^2/\nu$	$\leq 7.72 \times 10^6$
Hartmann number (*Ha*)	$B_{0z} r_{in}/\sqrt{\rho\mu_0\nu\eta}$	≤ 3778
Magnetic Prandtl Number (*Pm*)	ν/η	7.77×10^{-6}
Magnetic Reynolds Number (*Rm*)	$RePm$	≤ 40
Lundquist Number (*Lu*)	$Ha\sqrt{Pm}$	≤ 10
Azimuthal *Hartmann number* (Ha_ϕ)	$B_{0\phi}(r_{in}) r_{in}/\sqrt{\rho\mu_0\nu\eta}$	≤ 1259
Azimuthal *Lundquist Number* (Lu_ϕ)	$Ha_\phi\sqrt{Pm}$	≤ 3.51

Non-dimensional parameters of the DRESDYN MRI-experiment

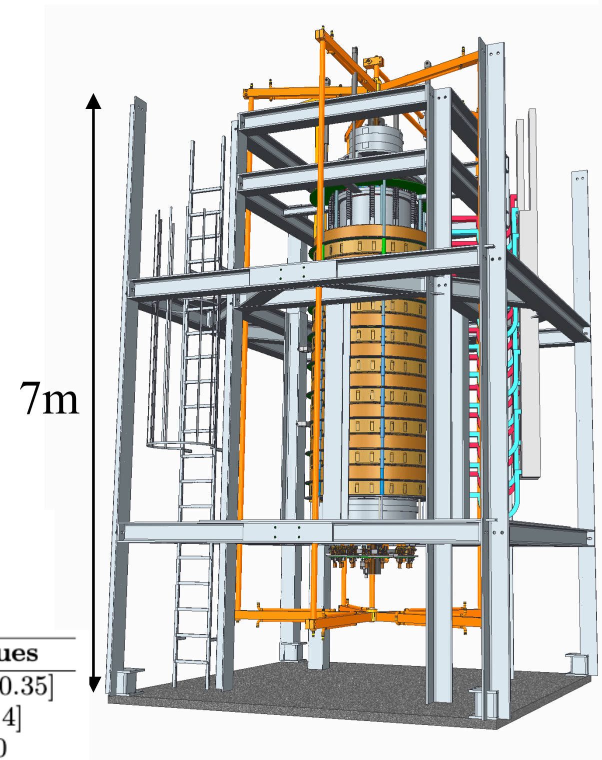

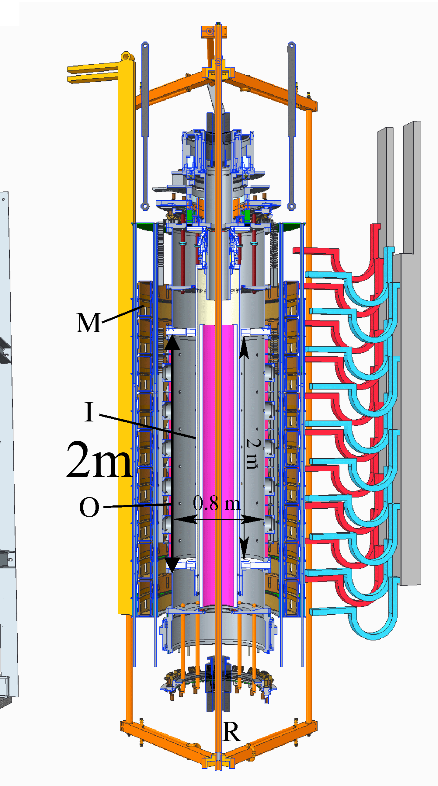

$Re \sim 10^6 - 10^7$

$Rm_{max} \sim 40$

$Lu_{max} \sim 10$

MRI regime achieved !

Main Goals:

- To study the linear and nonlinear dynamics of SMRI specifically for the upcoming DRESDYN-MRI experiment
- To understand the saturation mechanism of SMRI in the small-*Pm* regime
- To derive the dependence of the saturated SMRI amplitude with respect to different system parameters (*Rm, Lu, Pm,* ..)

Equations of non-ideal MHD equations

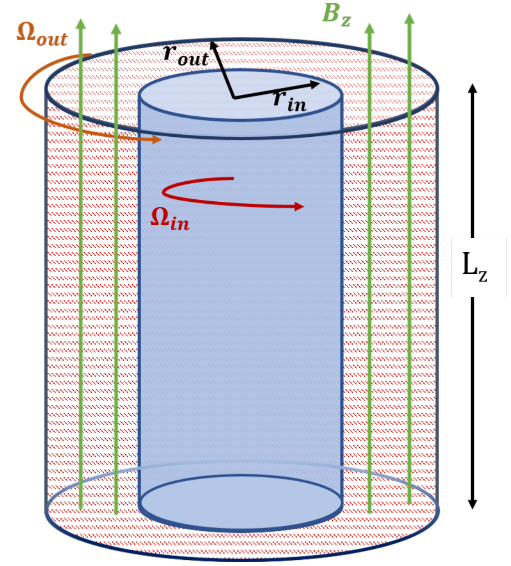

$$\partial_t \boldsymbol{U} + (\boldsymbol{U} \cdot \nabla \boldsymbol{U}) = -\frac{1}{\rho}\nabla P + \frac{1}{\rho\mu_0}(\nabla \times \boldsymbol{B}) \times \boldsymbol{B} + \nu \nabla^2 \boldsymbol{U}$$

$$\partial_t \boldsymbol{B} = \nabla \times (\boldsymbol{U} \times \boldsymbol{B}) + \eta \nabla^2 \boldsymbol{B}$$

$$\nabla \cdot \boldsymbol{U} = 0, \quad \nabla \cdot \boldsymbol{B} = 0$$

Equilibrium: $\mathbf{u}_0 = (0, r\Omega(r), 0), \quad \mathbf{B}_0 = (0, 0, B_{0z})$

$$\Omega(r) = \frac{r_{out}^2 \Omega_{out} - r_{in}^2 \Omega_{in}}{r_{out}^2 - r_{in}^2} + \frac{(\Omega_{in} - \Omega_{out})}{r_{out}^2 - r_{in}^2} \frac{r_{in}^2 r_{out}^2}{r^2}, \qquad \mu = \Omega_{out}/\Omega_{in} > 0.25 \text{ (Rayleigh-stable)}$$

Perturbations: $\mathbf{u} = \mathbf{U} - \mathbf{U}_0, \quad \mathbf{b} = \mathbf{B} - \mathbf{B}_0 \propto \exp(ik_z z + im\phi)$

Boundary conditions: no-slip for velocity
insulating for magnetic field

Pseudo spectral eigensolver based on Chebyshev decomposition

(Hollerbach & Rüdiger 2005)

Unstable regions in the Lundquist (Lu)- magnetic Reynolds (Rm) plane for **axisymmetric (m=0) SMRI** — 1D Linear Stability Results

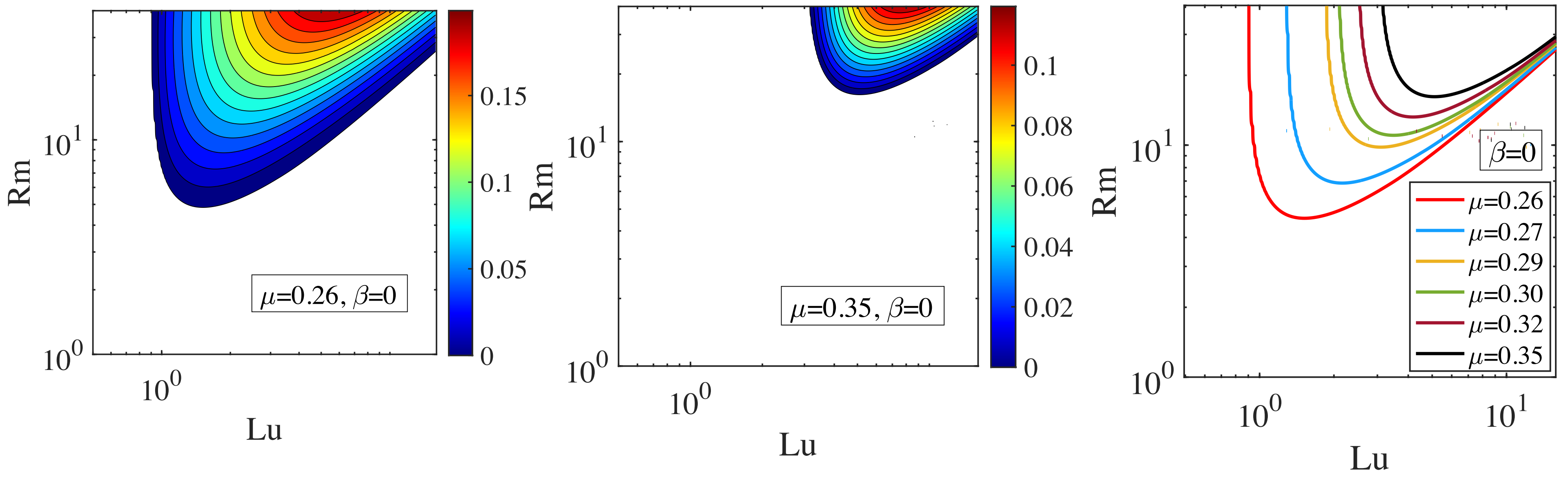

Mishra et al. 2022

SMRI can be well detected within the parameter regime achievable in the DRESDYN-MRI experiment, capturing its efficient growth range

Unstable regions in the Lundquist (Lu)- magnetic Reynolds (Rm) plane for **non-axisymmetric (m=1) MRI** — 1D Linear Stability Results

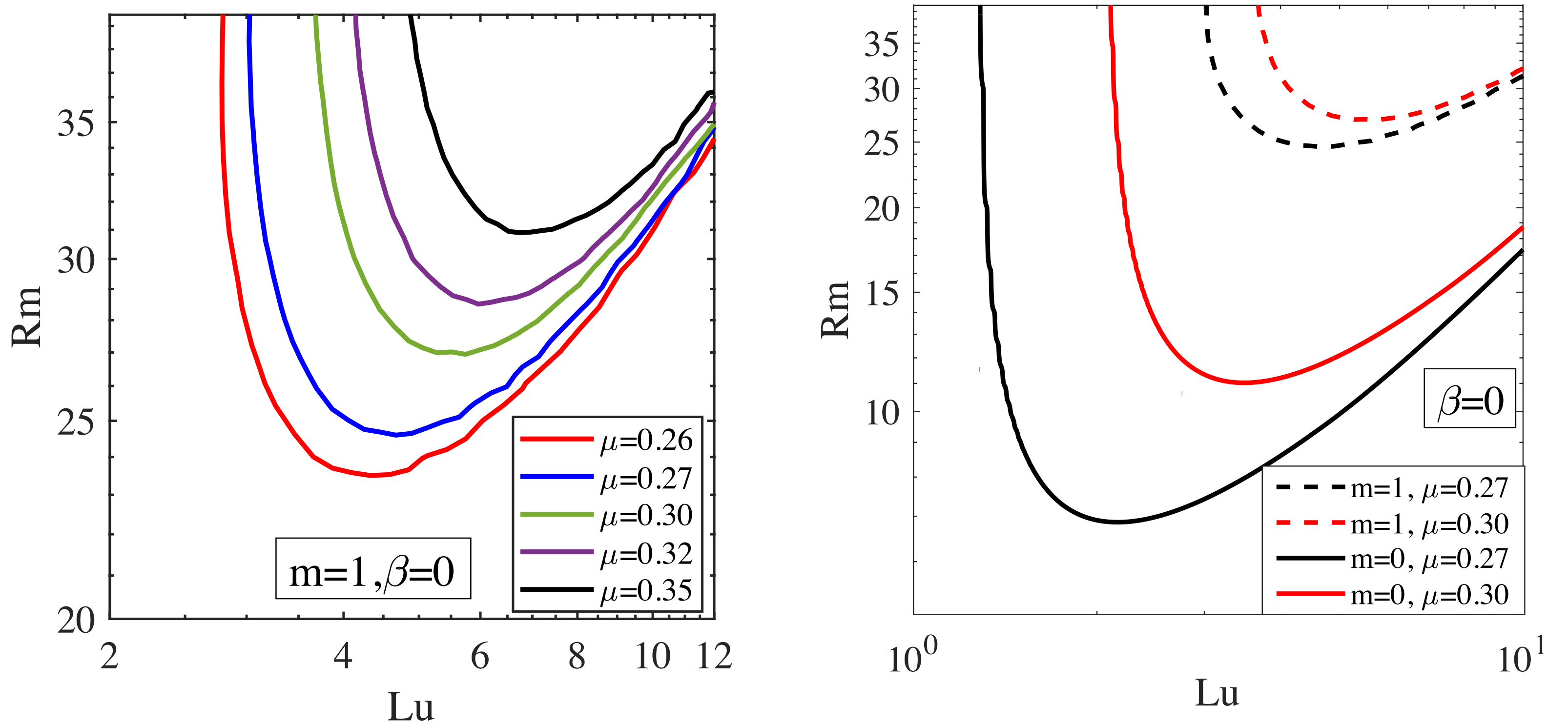

Mishra et al. 2024

SMRI can be well detected within the parameter regime achievable in the DRESDYN-MRI experiment, capturing its efficient growth range

SMRI: Nonlinear Saturation and Evolution

Points of Analysis

Mishra et al. 2023

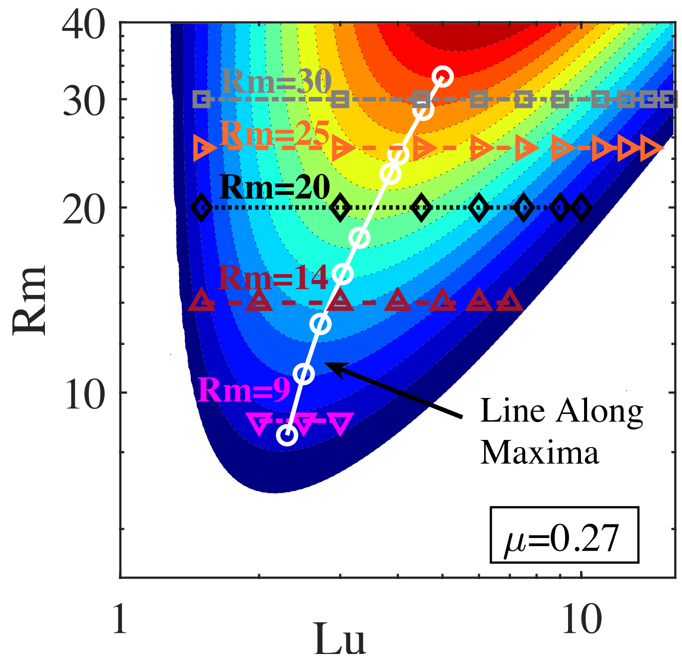

Instability region obtained from 1D linear stability analysis for $\mu = 0.27,\ Pm = 7.77 \times 10^{-6}$, and $k_{z,min} \geq 2\pi/L_z$

$$Re = [10^3,\ 4 \cdot 10^3,\ 7 \cdot 10^3,\ 10^4,\ 2 \cdot 10^4,\ 3 \cdot 10^4,\ 4 \cdot 10^4,\ 10^5]$$

We solved nonlinear MHD equations using pseudo-spectral code of Guseva et al. (2015)

Nonlinear evolution in the (r,z)-plane

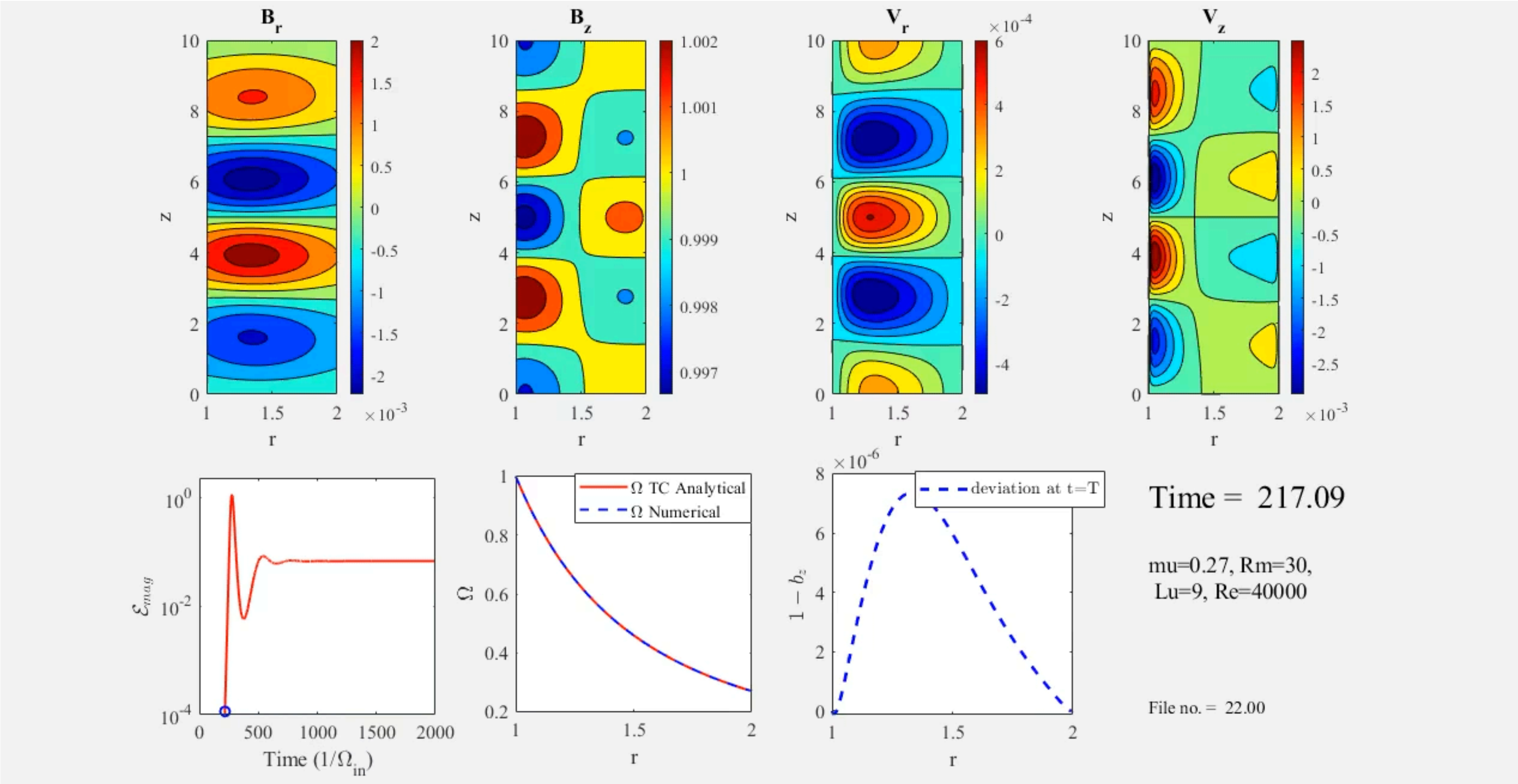

Saturation occurs via current sheet formation and resulting reconnection process

$$\mu = 0.27,\ Lu = 9,\ Rm = 30,\ Re = 4 \cdot 10^4$$

Energy saturation & dependence on Re

Mishra et al. 2023

Time evolution of the volume integrated magnetic energy

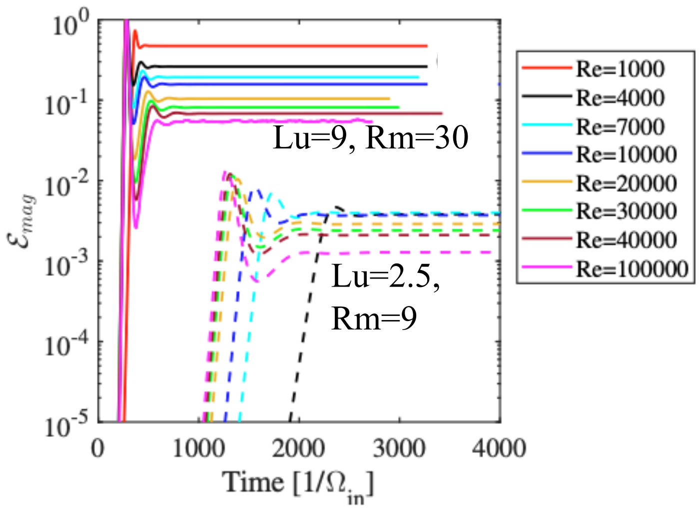

fitting: $Re^{-0.5}$

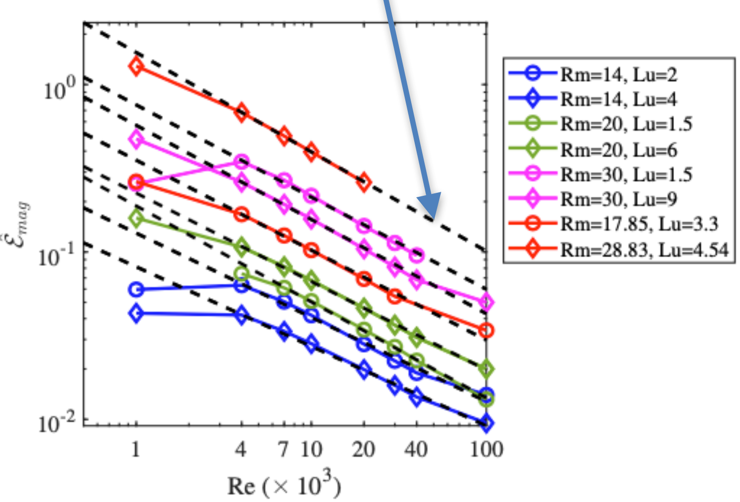

Saturated state magnetic energy as a function of Re

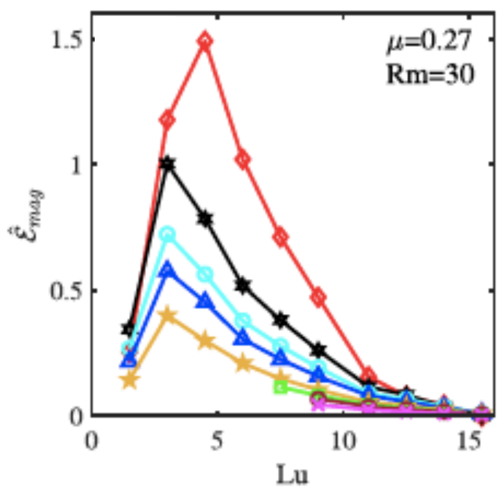

Dependence on *Lu*

Results: Torque & Dependence of turbulent torque on *Re*

Lu=9,
Rm=30

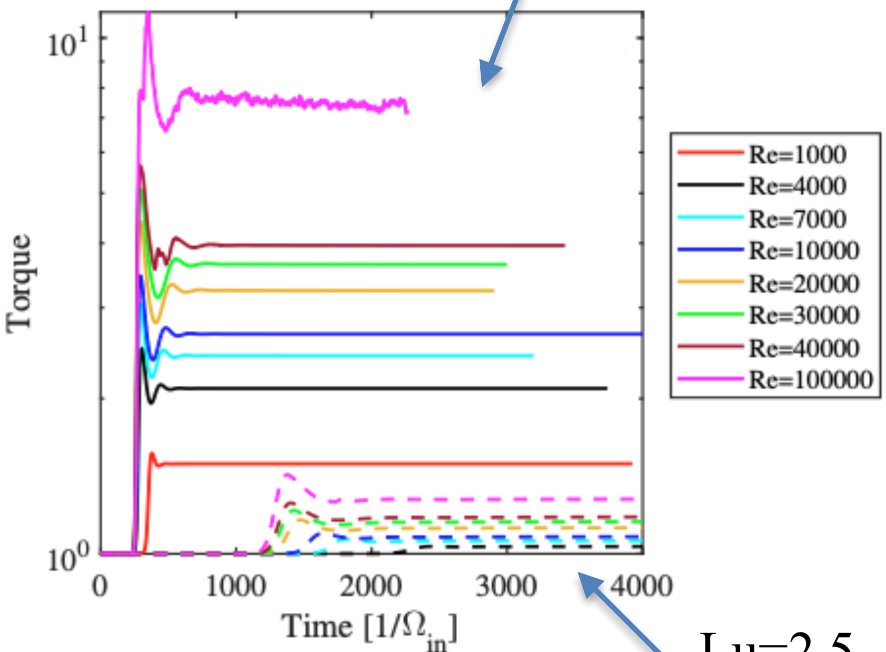

Lu=2.5,
Rm=9

Torque at the inner cylinder

fitting: $Re^{0.5}$

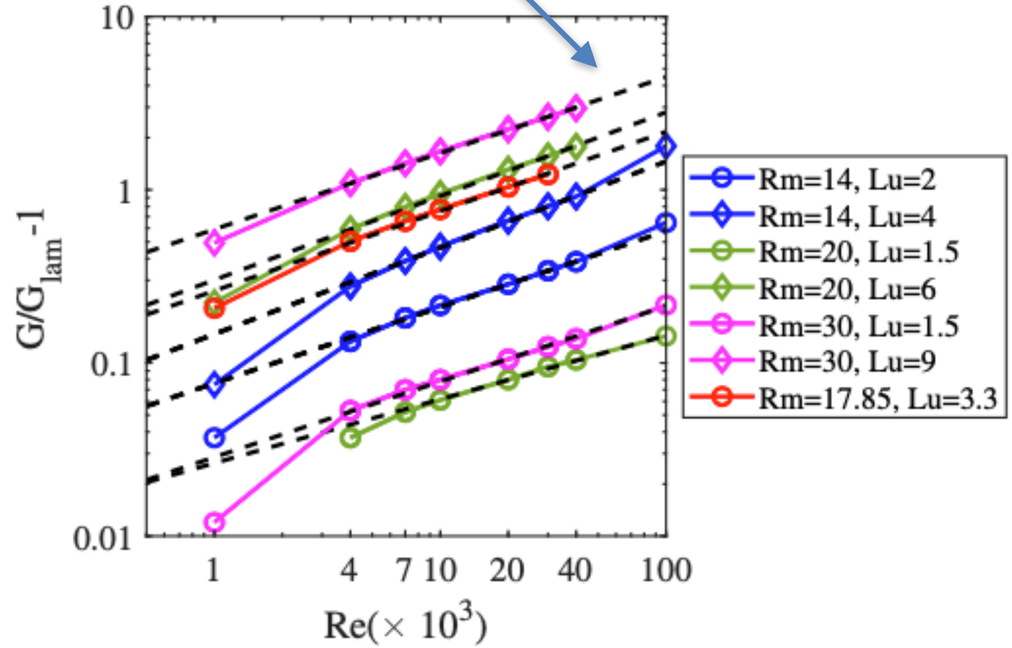

Normalised Turbulent Torque as a function of *Re*

$$G_{in,out} = -(r^3_{n,out}/Re)\int\int \frac{\partial}{\partial r}(u_\phi/r)d\phi dz$$

Mishra et al. 2023

Results: Amplitude of velocity and magnetic field perturbations

$\mu = 0.27$ (Lu, Rm)	u ($\Omega_{in} r_{in}$)	u (m/s)	b (B_0)	b (mT)
(2, 14)	0,0138	0,0808	0,0078	0,222
(4, 14)	0,0437	0,2560	0,0068	0,387
(1.5, 20)	0,0053	0,0443	0,0085	0,181
(6, 20)	0,0745	0,6234	0,0079	0,675
(1.5, 30)	0,0059	0,0740	0,0125	0,267
(9, 30)	0,1047	1,3142	0,1020	13,073

RMS velocity and magnetic field perturbations expected in the upcoming DRESDYN MRI-experiment (found by extrapolating power-laws to Re ~ 10^6)

Deviation of Ω from TC profile & local shear q

Mishra et al. 2023

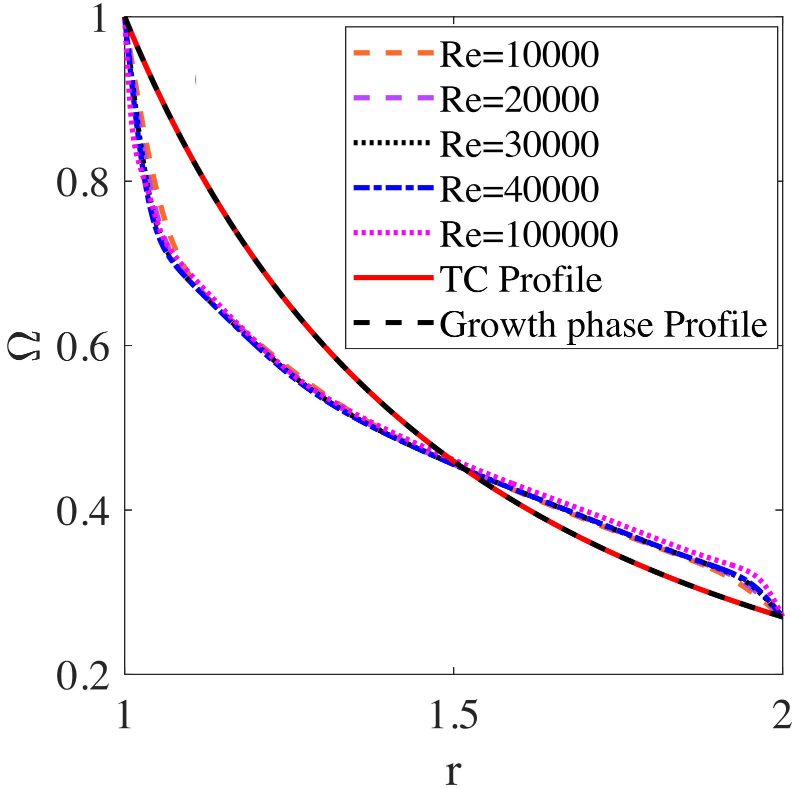

Rotation profile in saturated state

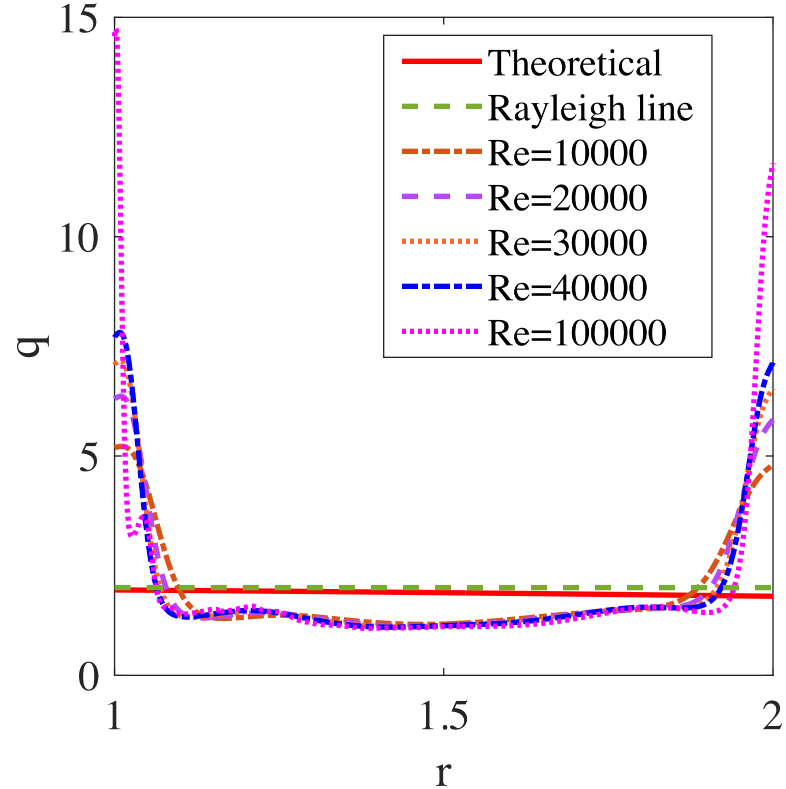

Local shear $q = -\frac{\partial ln\Omega}{\partial ln r}$ in saturated state

Non-axisymmetric Modes of SMRI: Nonlinear evolution

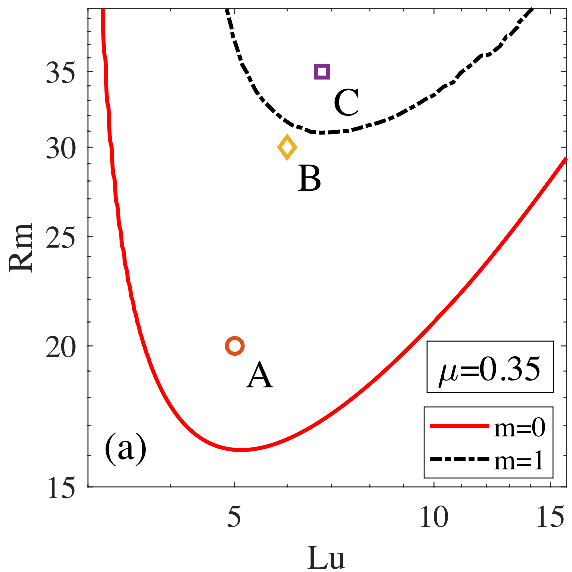

Linear instability in (Lu, Rm)-plane

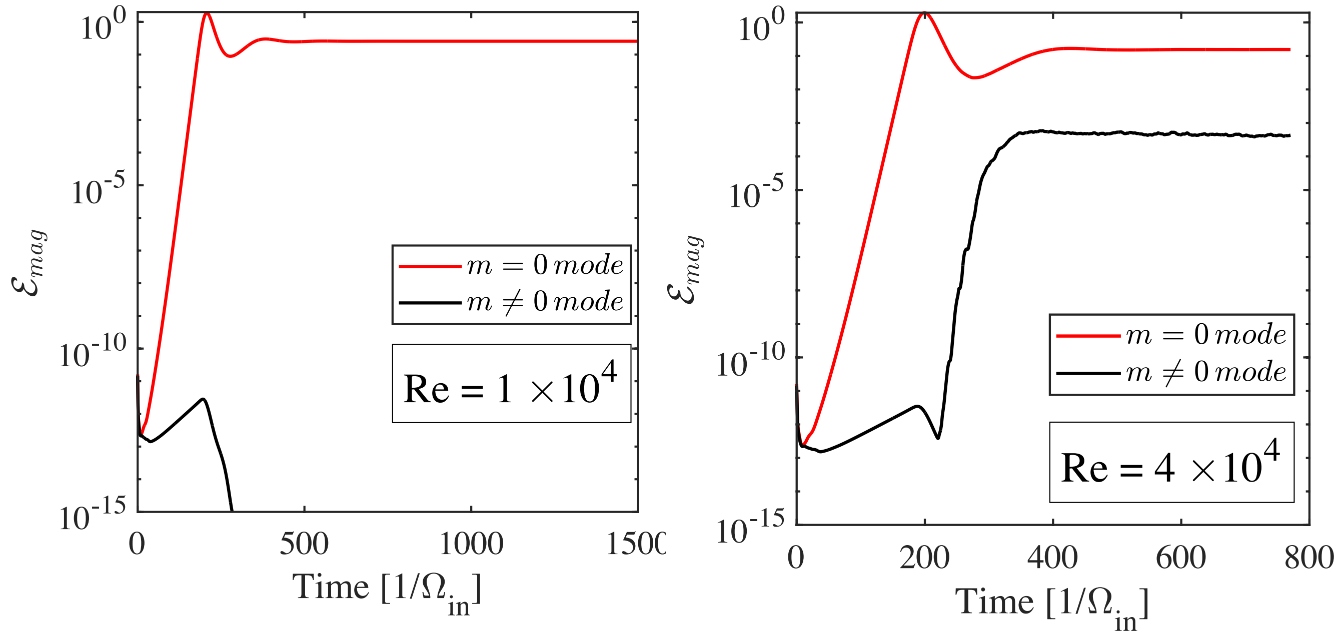

Evolution of magnetic energy at point C

Mishra et al. 2024

Non-axisymmetric Modes of SMRI: Nonlinear evolution

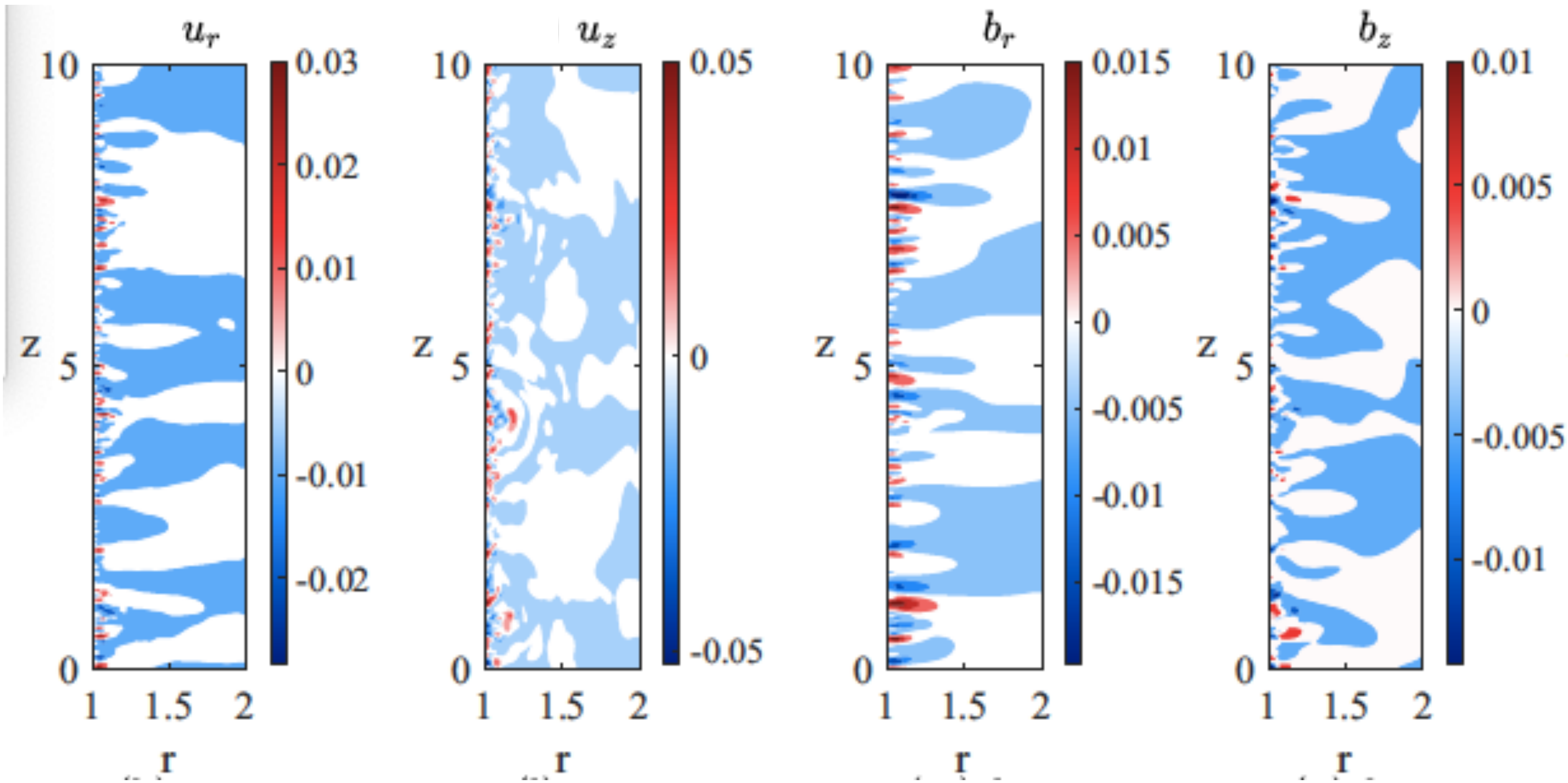

Mishra et al. 2024

Summary

- SMRI can be well detected within the parameter regimes achievable in the DRESDYN-MRI experiment, capturing its efficient growth range
- The nonlinear saturation occurs via magnetic reconnection process
- For different sets of (Lu, Rm), the magnetic energy in the saturate state and the normalized turbulent torque scales with $Re^{-0.5}$ and $Re^{0.5}$, respectively
- Magnitudes of velocity and magnetic field perturbation expected in the upcoming DRESDYN MRI-experiment were estimated

Please check out our papers on MRI in DRESDYN

Mishra, Mamatsashvili & Stefani, 2022, Phys. Rev. Fluids, **7**, 064802 (arXiv: 2112.01399)

Mishra, Mamatsashvili & Stefani, 2023, Phys. Rev. Fluids, **8**, 083902 (arXiv: 2211.10811)

Mishra, Mamatsashvili & Stefani, 2024, Phys. Rev. Fluids, **9**, 033904 (arXiv: 2307.16295)

Future work

- Investigation of MRI in finite-length cylinders in DRESDYN and Princeton experiments at small Pm << 1 and high $Re > 10^4$, taking into account the endcap effects: Ekman layers/circulations and Stewartson-Shercliff layers

- Onset, saturation and nonlinear evolution of SMRI under the influence of (insulating/conducting) endcaps in both MRI-experiments

- Dependence (scaling) of the saturated states on the system parameters (Lu, Rm, Pm, cylinder rotation rates, etc.)

- Detailed comparison with the experimental outcomes from DRESDYN and Princeton MRI-experiments

Thank you for your attention

This work was supported by Shota Rustaveli National Science Foundation of Georgia (SRNSFG) [#FR-23-1277]